Special Issue

Competing Reaction Pathways in Heterogeneously Catalyzed Hydrogenation of Allyl Cyanide: The Chemical Nature of Surface Species

Carsten Schröder,[a] Philipp A. Haugg,[a] Ann-Katrin Baumann,[a] Marvin C. Schmidt,[a] Jan Smyczek,[a] and Swetlana Schauermann*[a]

Abstract: We present a mechanistic study on the formation of an active ligand layer over Pd(111), turning the catalytic surface highly active and selective in partial hydrogenation of an α,β-unsaturated aldehyde acrolein. Specifically, we investigate the chemical composition of a ligand layer consisting of allyl cyanide deposited on Pd(111) and its dynamic changes under the hydrogenation conditions. On pristine surface, allyl cyanide largely retains its chemical structure and forms a layer of molecular species with the CN bond oriented nearly parallel to the underlying metal. In the presence of hydrogen, the chemical composition of allyl cyanide strongly changes. At 100 K, allyl cyanide transforms to unsaturated imine species, containing the C=C and C=N double bonds. At increasing temperatures, these species undergo two competing reaction pathways. First, the C=C bond become hydrogenated and the stable N-butylimine species are produced. In the competing pathway, the unsaturated imine reacts with hydrogen to fully hydrogenate the imine group and produce butylamine. The latter species are unstable under the hydrogenation reaction conditions and desorb from the surface, while the N-butylimine adsorbates formed in the first reaction pathway remain adsorbed and act as an active ligand layer in selective hydrogenation of acrolein.

Introduction

Controlling selectivity in chemical transformations of multi-unsaturated hydrocarbons is one of the most important challenges in modern heterogeneous catalysis. Specifically for the competing reaction pathways exhibiting only small differences in the activation barriers, the distribution of the products might be very broad and is difficult to control by using typical single-metal heterogeneous catalysts. Thus, a catalytic surface showing high activity for the desired reaction route might also greatly accelerate the unwanted reaction paths. A strategy to overcome this problem is to introduce a specific selective interaction between a reactant and a catalytically active site, which can govern the chemical transformations only into the desired direction. Such highly specific reactant/active site interactions are ubiquitous in enzymes[2] and have been successfully implemented into homogeneous catalysts through for example modification of an active metal site with specific organic ligands.[3]

Currently, a similar approach is being developed for heterogeneously catalyzed reactions by combining two functionalities inherent to heterogeneous and homogeneous catalysis: high activity of a catalytic metal surface and a specific interaction between the reactant and the active site, directing the chemical transformations towards the desired reaction route.[4] One of the most successful strategies within this approach is the functionalization of a catalytic surface with ligand-like adsorbates, for example organic adsorbates or covalently bonded functional groups, allowing for a selective promotion of the desired reaction pathway. Recently, such surface modification has gathered significant interest for the development of "ligand-directed" heterogeneous catalysis for a variety of reactions,[4b,e,5] in which the pre-adsorbed surface ligands induce specific adsorbate-adsorbate interactions with the reactant and by this turn the catalytic surface highly chemoselective. Thus, the deposition of n-alkanethiol onto Pd nanoparticles was reported to dramatically enhance the catalytic selectivity in 1-epoxy-3-butene selective hydrogenation on the olefinic bond from 10 to 94%.[4a] Kunz et al.[5b] reported that the modification of Pt nanoparticles with proline results both in strong increase of chemoselectivity in hydrogenation of acetophenon to phenylethanol and considerable raise of the conversion to almost 100%. Binghui at al[6] demonstrated that the presence of surface oleyamine array on PtCo nanocrystals leads to >90% selectivity towards C=O bond hydrogenation in α,β-unsaturated aldehydes containing both C=C and C=O double bonds. Recently, Medlin et al.[5f] demonstrated in a

[a] C. Schröder, P. A. Haugg, A.-K. Baumann, M. C. Schmidt, J. Smyczek, Prof. Dr. S. Schauermann
Institute of Physical Chemistry
Christian-Albrechts-University Kiel
Max-Eyth-Str. 2, 24118 Kiel (Germany)
E-mail: schauermann@pctc.uni-kiel.de

Special Issue Part of a Special Issue on Contemporary Challenges in Catalysis.

number of studies that "surface crowding" with thiolate-based self-assembled monolayers and other organic surface modifiers can be used to control the orientation of various multi-unsaturated reactants and considerably improve the selectivity towards the desired reaction pathway. Glorius et al.[7] reported significantly enhanced selectivity and activity in selective hydrogenation of acetophenone, trans-stilbene and phenylacetylene over Pd/Al_2O_3 and Ru/Al_2O_3 catalysts functionalized with N-heterocyclic carbens.

In our recent mechanistic studies[8] on chemoselective hydrogenation of an α,β-unsaturated aldehyde acrolein to unsaturated alcohol propenol over model Pd catalysts, we have shown that surface functionalization with ligands turns the catalyst highly active and nearly 100% selective toward the target product unsaturated alcohol. Specifically, it was shown that Pd(111) functionalized with allyl cyanide (AC) prior the reaction becomes highly active and selective toward the formation of the desired product propenol. In that study, we found indications that the chemical nature of the originally deposited AC dynamically changes under the reactive conditions – in presence of hydrogen and at elevated temperatures – allowing formation of a specific ligand layer, which enables acrolein adsorption in the desired adsorption geometry – via the O-end – and by this promotes its selective hydrogenation. The surface ligand species were identified as N-butylimine species, which remain stable under the reaction conditions applied for acrolein hydrogenation.[8]

While some aspects of the chemical transformation of AC on Pd(111) under the reaction conditions were addressed in the latter study, the full atomistic-level details of adsorption and reactivity behavior of AC under hydrogenation reaction conditions resulting in formation of an active ligand layer remain unknown. Specifically, AC is able to transform not only to N-butylimine species but also undergo alternative reaction pathways resulting in formation of the different partly hydrogenated surface species (e.g. amines). These competing processes might crucially affect the final composition of the surface turning over and by this decisively determine the overall efficiency of the catalyst. It appears feasible to control the surface composition of the ligand layer by tuning the pre-treatment and reaction parameter such, that mainly the desired ligand species would be produce and the competing reaction pathways of AC would be minimized. However, the control over the chemical composition requires detailed knowledge of the competing surface processes and how they specifically depend on the experimentally controllable parameters such as reaction temperature, AC coverage and hydrogen flux. This detailed information on these dependencies is not available at the moment. The main goal of this study is to obtain detailed atomistic-level understanding of the competing reaction pathways of AC under hydrogenation conditions resulting in formation of either the desired ligand layer (N-butylimine species) or the undesired side products of partial or full AC hydrogenation. Specifically, the effects of the experimentally controllable parameters, such as reaction temperature, presence of hydrogen and AC coverage, on the competing surface processes need to be explored, which will allow to prepare tailor-made active ligand layers with the desired catalytic properties.

Previously adsorption behavior of structurally similar molecules – simple nitriles and isocyanides – was addressed by a variety of surface sensitive spectroscopies on pristine transition metal surfaces.[9] Specifically, two possible adsorption configurations – η_1(N) or η_2(N,C) – were proposed for acetonitrile,[9d,j] methyl isocyanide,[9g,k] azomethane,[9l] HCNH[10] and HCN[9m] adsorbed on Pt(111), methyl isocyanide and acetonitrile[9f] on Pd(111), acetonitrile on TiO_2-supported Au,[9i] methyl isocyanide on Rh(111)[9e] and HCNH on Ru(001).[9h] In the η_1(N) configuration, the N atom directly interacts with the underlying metal, while the nearest C atom is attached only to N. In the η_2(N,C) configuration, both N and the nearest C establish bonds to the underlying metal surface. Adsorption and reactivity behavior of these compounds on H-containing transition metal surfaces and/or under hydrogenation reaction conditions at elevated temperatures was not yet investigated in surface science studies to the best of our knowledge.

To obtain a deeper microscopic understanding of the processes resulting in the formation of the active ligand layer, we performed a comprehensive spectroscopic study on adsorption and reactivity behavior of AC on pristine and H-containing Pd(111) surface. A combination of infrared reflection absorption spectroscopy (IRAS) and molecular beam techniques was employed in this study in a broad range of temperature and coverage conditions. Specifically we show, that on the pristine Pd(111) surface at 100 K AC adopts an adsorption configuration with the CN-entity oriented nearly parallel to the surface, while the C=C bond is tilted with respect to the surface plane. With increasing temperature, the spectroscopic observations suggest a strong rehybridization of the C=C bond resulting in formation of either π- or di-σ bonded adsorbates on pristine Pd(111). The presence of co-adsorbed H dramatically changes both the chemical structure and the adsorption configuration of originally adsorbed AC. Already at the lowest investigated temperature (100 K), molecular AC transfers to butylimine species, in which a C=N entity is formed exhibiting a characteristic vibrational band at 1755 cm^{-1}. At elevated temperatures, the imine adsorbates can undergo two competing reaction pathway: *(i)* one resulting in hydrogenation of the C=C bond and leading to formation of strongly bound saturated imine adsorbates (N-butylimine species); *(ii)* the other resulting in a stepwise hydrogenation of the C=C and the C=N bonds and formation of the saturated amine species, which can desorb as molecular butylamine. The saturated N-butylimine species formed in the first reaction pathway was found to be stable under the reaction condition and form an active ligand layer governing chemoselective acrolein hydrogenation. The amine species formed in the second pathway are unstable and readily desorb in presence of hydrogen. Obtained results provide important atomistic-level details on chemical transformations of AC under the hydrogenation reaction conditions, which play a key role in formation of active ligand layers in ligand-directed heterogeneous catalysis.

Experimental Section

All experiments were performed in an ultrahigh vacuum (UHV) apparatus combining molecular beam techniques, IRAS and quadrupole mass spectrometry (QMS). The apparatus is equipped with a dedicated preparation chamber, which is separated from the experimental chamber by an UHV gate valve. After preparation, the sample can be transferred from the preparation to the experimental chamber without breaking the vacuum. Both chambers are operating at a base pressure $< 2.0 \cdot 10^{-10}$ mbar. Full details on the apparatus design can be found elsewhere.[11]

The Pd(111) single crystal (10×10 mm, MaTeck GmbH) was cleaned prior to use in the preparation chamber by repeated cycles of Ar^+ ion bombardment at room temperature, followed by annealing at 1100 K and subsequent oxidation in $1 \cdot 10^{-6}$ mbar O_2 at 700–750 K. The last step contains the rapid flash of the sample to 900 K. Shortly before each experiment the sample was flashed to 600–800 K before cooling to the required temperature to remove CO adsorbates. The long range order and cleanliness of the Pd(111) single-crystal were checked by Low Energy Electron Diffraction (LEED), Auger Electron Spectroscopy (AES) and additionally by IRAS of adsorbed CO to probe the abundance of adsorption sites. Allyl cyanide (Sigma-Aldrich, 98%) was purified with multiple pump-freeze-thaw cycles before each experiment. Hydrogen (Linde HiQ 6.0) was used without any further purification.

Two doubly differentially pumped effusive molecular beams were used for dosing the molecules onto the surface. Typical flux rates were $8.5 \cdot 10^{14}$ molecules$\cdot$cm$^{-2}\cdot$s^{-1} for H_2 and $7.2 \cdot 10^{12}$ molecules$\cdot$cm$^{-2}\cdot$s^{-1} for allyl cyanide. The IRAS data were obtained using a vacuum Fourier transform infrared (FTIR) spectrometer (Bruker Vertex 80v) with a spectral resolution of 2 cm^{-1} combined with a mid-infrared (MIR) polarizer and using p-polarized IR light. The spectrometer was equipped with a narrow band Mercury-Cadmium-Telluride (MCT) detector.

The deposition of molecules as well as the evolution of reaction products was monitored by a quadrupole mass spectrometer (QMS) (Hiden HAL 301/3F). A detailed description of the setup can be found elsewhere.[11]

The vibrational spectra were calculated at the B3LYP level with the aug-cc-pvqz basis set of a single molecule in the gas phase using the Gaussian16 software.[12] The computed frequencies were used to assign the specific vibrational modes to the experimentally measured vibrational frequencies of the unperturbed molecules adsorbed in the multilayer coverage regime.

Results and Discussion

Adsorption of AC was investigated on well-defined Pd(111) surface under UHV conditions in the temperature range 100–250 K by combination of IRAS and molecular beam techniques. The surface coverage was varied in a broad range – from submonolayer to multilayer coverages. The spectra obtained for AC multilayers at 100 K were used as a reference for molecular species, which are not perturbed by the direct interaction with the underlying metal surface. The assignment of the experimentally observed vibrational band was performed by comparison of these spectra with the known gas phase spectra[13] and theoretical calculations performed in this study.

Assignment of vibrational bands in allyl cyanide

Figure 1 shows multilayer IR spectra of AC obtained at 100 K during increasing exposure (1–4) and a theoretical spectrum (5) resulting from harmonic B3LYP/aug-cc-pvqz gas phase calculation using the Gaussian16 software.[12] At this temperature, a simultaneous continuous growth of all vibrational bands was observed, which is characteristic for the formation of multilayers. The calculated IR spectrum was corrected by a factor of 0.965, scaled on the ν(C=C) vibrational band at 1648 cm^{-1}, which can be clearly identified in the experimentally measured multilayer spectra. A detailed assignment of all vibrational bands, based on the harmonic B3LYP gas phase frequency calculation, is summarized in Table 1. The last column of this table also shows the references to the previously published reports that were used for additional verification of the assignment made in this study.

There is a good agreement in spectral position as well as simulated intensities of the calculated spectra compared to the experimental data, which provides a sufficient level of accuracy for comparison of theoretically computed and experimentally measured spectra. In the region of the C–H stretch vibrations, the IR bands are observed at 3093 ($\nu_{as}(=CH_2)$), 3032 (ν(=CH)) and 2990 ($\nu_s(=CH_2)$) cm^{-1}, which can be assigned to the asymmetric and symmetric =C–H stretching modes containing the olefinic C atom. The C–H stretching vibrations related to the aliphatic –CH_2– entity exhibit lower vibrational frequencies: at 2940 ($\nu_{as}(CH_2)$) and 2918 ($\nu_s(CH_2)$) cm^{-1}. The nitrile stretching vibration ν(C≡N) is observed at 2250 cm^{-1} with a small shoulder at 2265 cm^{-1}, which can be related to intermolecular interactions of AC in the multilayer ice as previously shown in experimental spectroscopic[13b] and theoretical studies.[13a] Specifically, it was reported that the nitrile stretching vibration ν(C≡N) is highly sensitive to the chemical surrounding. Thus, the IR experiments of Getahun et al.[14] on nitrile containing amino acids in water and tetrahydrofuran (THF) solvent show a frequency blue-shift of up to 10 cm^{-1} when THF was replaced by water. A similar trend was reported by Lindquist et al.[15] in a theoretical study on acetonitrile/water and acetonitrile/THF clusters. The very sharp band at 1648 cm^{-1} can be assigned to the ν(C=C) stretching vibration. The assignment of the stretching vibrations ν(CH_x), ν(C≡N) and ν(C=C) are in good agreement with previously reported assignment performed in the studies on gaseous, liquid and solid AC by Durig[13a] and Verma.[13b]

The intense band at 1419 cm^{-1} is related to the asymmetric deformation vibration $\delta_{as}(CH_2)$ of the methylene group. A small shoulder visible at 1402 cm^{-1} can be assigned to the in plane deformation vibration $\delta_{ip}(=CH_2)$ of the terminal vinyl group. The vibrational band at 1325 cm^{-1} is typical for the symmetric deformation vibration $\delta_s(CH_2)$ of the methylene group. The band at 1296 cm^{-1} is assigned according to the calculations to the in-plane bending vibration $\delta_{ip}(=CH)$ of the C–H bond with carbon being involved in the olefinic group. Previously, the bands at similar frequencies 1287 and 1294 cm^{-1} were reported by Verma et al.[13b] for solid AC adsorbed on CsBr plate at 90 K

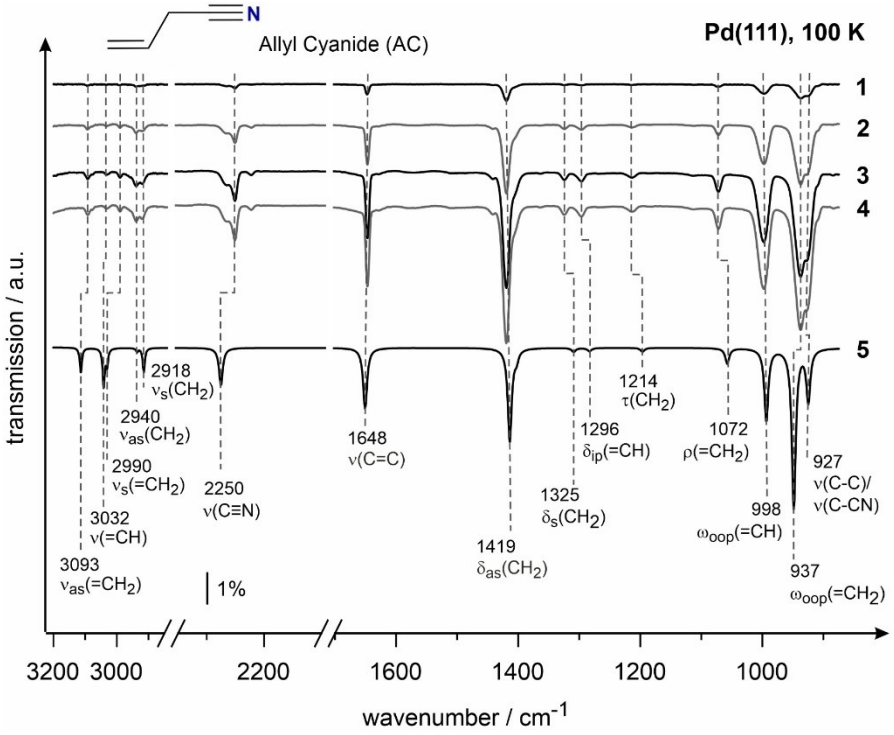

Figure 1. IR spectra of allyl cyanide (AC) obtained at 100 K on Pd(111) in the multilayer coverage range. AC was dosed at a flux of $1.0 \cdot 10^{14}$ molecules $\cdot cm^{-2} \cdot s^{-1}$. Allyl cyanide exposures: (1) $6.0 \cdot 10^{15}$, (2) $3.0 \cdot 10^{16}$, (3) $4.2 \cdot 10^{16}$, (4) $5.4 \cdot 10^{16}$ molecules $\cdot cm^{-2}$. The spectrum (5) results from theoretical calculation by using B3LYP-aug-pvqz gas phase calculation of allyl cyanide with a correction factor of f = 0.965.

Table 1. Assignments of vibrational modes of allyl cyanide and its partly hydrogenated derivatives. ν: stretching, δ: deformation, τ: twisting, ρ: rocking, ω: wagging, γ: scissoring vibrations.

Frequency [cm^{-1}] Multilayer (100 K)	Sub monolayer (140 K)	Sub monolayer (H_2, 250 K)	Theoretically calculated spectrum (B3LYP / aug-cc-pvqz, f = 0.965)	Assignment	Ref.
3093			3113	$\nu_{as}(=CH_2)$	[13]
3032			3040	$\nu(=CH)$	[13a]
2990			3030	$\nu_s(=CH_2)$	[13a]
2940			2935	$\nu_{as}(-CH_2)$	[13a]
2918			2914	$\nu_s(-CH_2)$	[13b]
	2879			$\nu_{as}(-CH_x)$	[18]
	2864			$\nu_s(-CH_x)$	[18]
2250			2275	$\nu(C\equiv N)$	[13]
		1755		$\nu(C=N)$	[9d,f,k, 22]
1648	1648		1650	$\nu(C=C)$	[13]
		1608, 1580		$\delta(NH_2)$	[9 h,m, 24,25]
1419	1419		1413	$\delta_{as}(CH_2)$	[13]
1402			1402	$\delta_{ip}(=CH_2)$	[13b]
1325			1308	$\delta_s(CH_2)$	[13]
1296			1282	$\delta_{ip}(=CH)$	[13a]
		1275		δ(HNC)	[9 l, 10, 20]
1214			1196	$\tau(CH_2)$	[13a]
1072			1057	$\rho(=CH_2)$	[13a]
998	990		993	$\omega_{oop}(=CH)$	[13b]
937	934		948	$\omega_{oop}(=CH_2)$	[13a]
927	915		924	$\nu(C-C)$/ $\nu(C-CN)$	[13]

and at 1285 cm^{-1} for liquid AC. Durig assigned the band at 1300 cm^{-1} measured in gaseous and at 1288 cm^{-1} in solid AC to the same $\delta_{ip}(=CH)$ vibrational mode.[13a] This slight difference between 1296 cm^{-1} observed in our study and 1288 cm^{-1} reported for solid AC by Durigmay be related to intermolecular interactions in the multilayer AC ice.

The weak band at 1214 cm^{-1} is related to the twisting vibration $\tau(CH_2)$ of the methylene group. The vibrational band

at 1072 cm^{-1} can be assigned to the rocking vibration of the vinyl group $\rho(=CH_2)$ according to our calculations. Previously, Durig et al.[13a] reported the band at 1066 cm^{-1} in the gas phase, 1070 cm^{-1} in the liquid phase and 1075 cm^{-1} in solid AC and assigned them to the same rocking vibration of the vinyl group $\rho(=CH_2)$. On the other hand, Verma et al.[13b] assigned a band at 1070 cm^{-1} measured for liquid AC to a combination vibration of a valence and torsion vibration of the C–C≡N entity. The very intense bands at 998 ($\omega_{oop}(=CH)$) and 937 cm^{-1} ($\omega_{oop}(=CH_2)$) are assigned to the out-of-plane wagging vibrations of the vinyl hydrogens. Both assignments are in a good agreement with the assignment of Durig et al.,[13a] while Verma assigned the vibration at 936 cm^{-1} in liquid AC and 947 cm^{-1} in solid AC to the stretching mode of the C–C≡N entity (ν(C–C≡N)). The same author assigned the vibration at 906 cm^{-1} in liquid AC to out-of-plane wagging mode of the vinyl hydrogen.[13b] Based on our calculations, the vibration at 927 cm^{-1} can be assigned to a mixed mode of the ν(C–C≡N) and ν(C–C) stretching vibrations, which rather agrees with the assignment suggested by Durig.[13a]

Generally, the previous assignments of the vibrational bands of AC performed by Durig and Verma can be confirmed with just a few exceptions related to the low-frequency range, in which contradictory assignments were suggested by these two groups. A detailed visualization of the most prominent and for further discussion most important vibrational bands are shown in Figure 2. The blue arrows show the displacement vector of the individual atoms involved in each vibrational mode, while the gold arrow displays the resulting dynamic dipole moment. The arrow related to the resulting dynamic dipole moment is arbitrarily placed in the center of mass of AC. In the following, the orientation of the dynamic dipole moments with respect to the metal surface plane will be discussed for the selected vibrations. On metal surfaces, only those vibrational modes are visible in IR spectra, whose dynamic dipole moment has a non-zero projection onto the surface normal as a consequence of the metal surface selection rule (MSSR).[16] Consequently, the absence of certain IR vibrational peaks indicates that the related bonds are oriented nearly parallel to the surface and therefore not visible. It should be also kept in mind that the geometrical structure of adsorbed species might significantly differ from the alone-standing unperturbed molecules shown in Figure 2.

IR spectra of allyl cyanide adsorbed on Pd(111) at 100 K: coverage dependence

Having identified the vibrational modes in the multilayer, we studied adsorption of AC as a function of coverage to obtain detailed understanding of the chemical nature and the adsorption geometry of molecular species closely interacting with Pd surface. Figure 3 shows the IR spectra recorded on pristine Pd(111) at 100 K after successive exposure to AC in the range $7.2\cdot10^{13}$ to $4.3\cdot10^{15}$ molecules·cm^{-2}. Importantly, the highest AC coverage corresponds to a few monolayers, which allows us to directly follow the evolution of the individual vibrational bands starting from sub-monolayer to multilayer coverage. This approach ensures a univocal assignment of the vibrational bands detected at submonolayer coverages by direct comparison with the bands observed for multilayers, whose assignment was discussed in the previous section (Figure 1).

At the lowest coverage (Figure 3 spectra 1 and 2), only one vibrational band at 1419 cm^{-1} is visible in the spectra, which is related to the asymmetric deformation vibration of the methylene group $\delta_{as}(CH_2)$. This observation indicates that AC adopts a flat lying adsorption geometry with both the nitrile and vinyl group being oriented parallel to the surface. The presence of the vibrational band at 1419 cm^{-1} further indicates that the original geometric structure of AC becomes strongly perturbed upon adsorption on the metal surface. The dynamic dipole moment of the $\delta_{as}(CH_2)$ vibration lies in the same plane as the dynamic dipole moments of the C≡N and C=C stretching

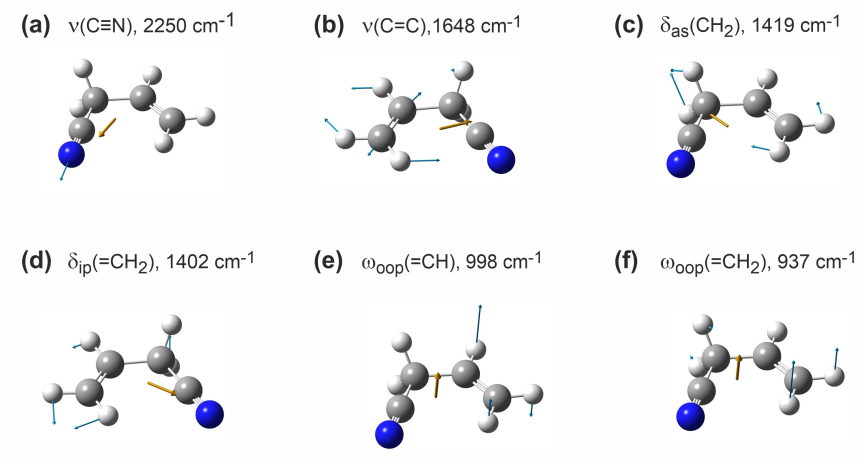

Figure 2. Visualization of selected vibrational modes of allyl cyanide in the gas phase using GaussView 6.1.[1] Blue arrows indicate the displacement vector of the individual atoms involved in the vibrational mode, gold arrows show the resulting dynamic dipole moment vector of the corresponding mode.

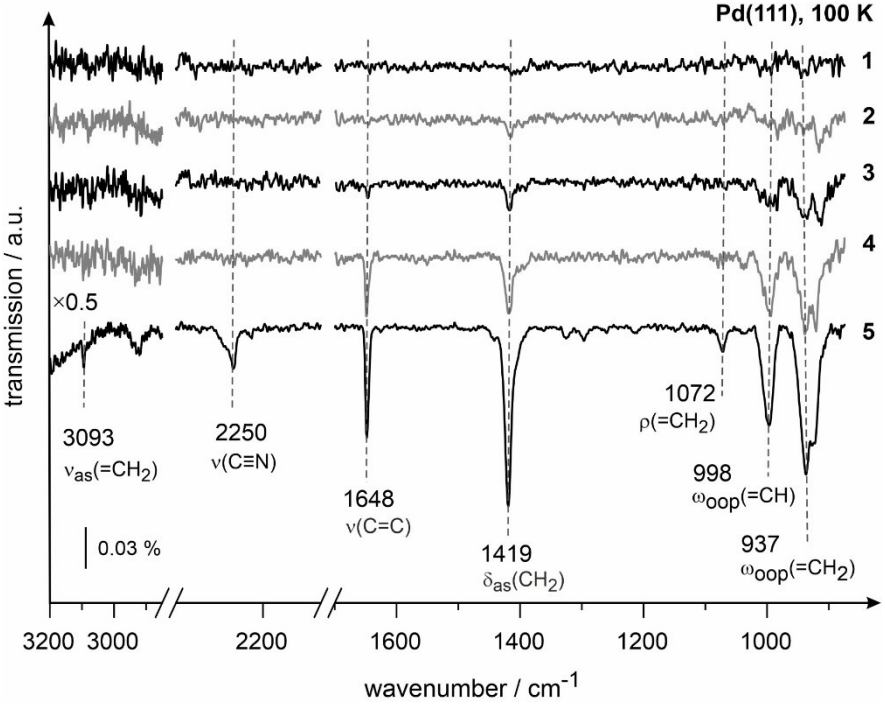

Figure 3. IR spectra of AC obtained at 100 K on Pd(111) in sub- and multilayer coverage range. AC was dosed at a flux of $7.2\cdot10^{12}$ molecules·cm^{-2}·s^{-1}. AC exposures: in (1) $7.2\cdot10^{13}$, (2) $2.9\cdot10^{14}$, (3) $3.6\cdot10^{14}$, (4) $7.2\cdot10^{14}$, (5) $4.3\cdot10^{15}$ molecules·cm^{-2}

vibrations for the gaseous AC (Figure 2). The fact, that the latter two vibrations are not seen in the infrared spectra suggests that the related bands are oriented nearly parallel to the surface and not visible due to MSSR. If the geometrical structure of AC would be retained upon adsorption, also the band at 1419 cm^{-1} ($\delta_{as}(CH_2)$) would be invisible due to the same effect. Since this band is observed in the adsorbed AC, the related dynamic dipole moment must be inclined with respect to the plane containing the C=C and C≡N bonds (see Figure 2). Most likely, this means that the H atoms of the -CH_2-group become lifted above the surface, so that the resulting dynamic dipole moment of $\delta_{as}(CH_2)$ vibration is inclined with respect to the C=C/C≡N plane and the plane of the metal surface. With increasing AC coverage, the band at 1419 cm^{-1} grows in intensity and a band at 1648 cm^{-1} appears in spectrum 3, which is related to the C=C stretching vibration ν(C=C). Simultaneously, the bands at 998 ($\omega_{oop}(=CH)$) and 937 cm^{-1} ($\omega_{oop}(=CH_2)$) related to wagging vibrations of the vinyl group evolve. The spectrum 5 obtained at the highest exposure $4.3\cdot10^{15}$ molecules·cm^{-2} contains three additional bands at 3093 ($\nu_{as}(=CH_2)$), 2250 ($\nu(C\equiv N)$) and 1072 cm^{-1} ($\rho(=CH_2)$). Taking into account the density of surface Pd atoms on Pd(111), which amounts to $1.5\cdot10^{15}$ atoms·cm^{-2}, and assuming that the sticking coefficient of AC is close to unity at 100 K, it might be concluded that the transition from the (sub-)monolayer to multilayer coverage occurs approximately between the spectra 2 and 4. In our previous STM studies,[8] adsorption of AC was investigated on a pristine Pd(111) surface in a broad range of temperature conditions. Based on the adsorption model developed for pristine Pd(111), the space demand for a single AC molecule was estimated to be approximately 8.5 Pd atoms. Assuming this space requirement, we estimate the saturation coverage of AC laying in the range $1.6\cdot10^{14}$–$1.8\cdot10^{14}$ molecules·cm^{-2}, which roughly correspond to the spectra 1 and 2 in Figure 3. In this case, in might be concluded that when adsorbed below the monolayer coverage, most of AC surface species are lying flat on the surface with the C=C and C≡N bonds being oriented close to parallel to the underlying metal and therefore invisible in IRAS due to MSSR.[16] Upon transition to the second and the further layers, the newly incoming molecules adopt a random orientation with respect to the surface, so that first the C=C and then the C≡N bonds become visible.

At sub-monolayer coverages (spectra 1–2), the absence of both vibrational bands related to out-of-plane wagging vibrations of the vinyl hydrogens ($\omega_{oop}(=CH)$ and $\omega_{oop}(=CH_2)$) at 998 and 937 cm^{-1} may indicate that the vinyl group undergoes strong rehybridization losing the π-bond character. There are two limiting types of interactions usually discussed in the literature:[17] a strong di-σ-interaction resulting in a rehybridization of both carbon atoms and a weaker π-bonded type of interaction. If the C=C bond would be preserved and participate in a π-type bonding, either the out-of-plane wagging (ω_{oop}-(=CH) at 988 and $\omega_{oop}(=CH_2)$ at 937 cm^{-1}) or in-plane deformation ($\delta_{ip}(=CH_2)$ at 1402 cm^{-1}) vibrations of the olefinic hydrogen atoms would be expected to be visible in the infrared spectra, which is not the case. On the other hand in case of a di-σ-bonding, one could expect the appearance of new or spectrally shifted vibrational bands in the region of CH stretching or CH deformation vibrations, which was either not observed here. Based on the available experimental data, it seems not to be

possible to distinguish between these two conceivable bonding types. At increasing coverages (spectra 3–5), all bands related to the C=C bond – 1648, 998 and 937 cm^{-1} – become visible in the spectra, pointing to a lesser extent of the olefin bond perturbation in the high coverage regime. A similar coverage-dependent change of the adsorption configuration from a di-σ bonding at low coverages to a π-complex at higher coverages have been reported by Lee et al.[18] in an IRAS adsorption study of C4-olefins on Pt(111) at 80 K.

Previously, adsorption behavior of simplest types of nitriles and isocyanides, such as HCN, acetonitrile and methyl isocyanide, was investigated in surface science studies on a variety of metals.[9a,c–g,i–k,m,19] Koerdsch et al. investigated the adsorption behavior of HCN on Pd(111) in a combined high resolution energy loss spectroscopy (HREELS) performed in an off-specular mode and temperature programmed desorption (TPD) study.[9a] The authors proposed a di-σ bonded η_2(C,N) adsorption configuration for the C=N bond, in which the formed nitrile groups show an imine character as concluded based on the observed strong frequency shift from 0.259 meV (2089 cm^{-1}) to 0.191 meV (1540 cm^{-1}). The NEXAFS study by the same authors confirmed this conclusion by showing that the C–N axis is oriented parallel to the surface.[9b] In a more recent IRAS study on acetonitrile and methyl isocyanide adsorbed on Pd(111) at 80 K, Murphy et al. reported a close to parallel orientation of the isocyanide group at low coverages and a more upright η_1(C)-configuration in the higher coverage regime.[9f] In this study, a prominent shift of the nitrile stretching vibration from 2249 to 1755 cm^{-1} was observed for acetonitrile, which was explained by a strong weakening of the nitrile group due to interaction with the underlying Pd. This considerable shift was interpreted as a consequence of a strong rehybridization of the related orbitals and formation of a η_2(C,N) adsorption configuration of the original nitrile groups, in which the original triple C≡N bond rather turns to double C=N imine bond. In a combined EELS and TPD study by Avery et al.[9g] on adsorption of methyl isocyanide on Pt(111), two types surface species were suggested: *(i)* a terminally bonded species observed at low coverage with a characteristic vibrational band at 2265–2240 cm^{-1} and *(ii)* an imine-like species observed at higher coverages, exhibiting a vibrational band in the range 1600–1770 cm^{-1}. In the same group, the adsorption of acetonitrile was investigated on Pt(111) by a combination EELS, X-ray photoelectron spectroscopy (XPS) and TPD,[9d] in which an η_2(C,N)-configuration was deduced for acetonitrile, showing the characteristic vibrational band at 1615 cm^{-1} in the typical imine region (ν(C=N)). A similar imine-related vibrational band at 1660 cm^{-1} was also observed in an IR study by Szilágyi et al.[9c] on acetonitrile and methyl isocyanide adsorption on Pt(111)/SiO_2. In a combined EELS, Auger electron spectroscopy (AES) and TPD study by Semancik et al.[9e] on adsorption of methyl isocyanide on Rh(111), two different adsorption species were reported: *(i)* a low-coverage species, exhibiting a vibrational band at 1710 cm^{-1}, which were assigned to a bridged-bonded geometry, and *(ii)* a second type of species related to the high coverage range, showing a vibrational band at 2170 cm^{-1} and interpreted as on-top bonded species. Friend et al.[19] investigated acetonitrile and methyl isocyanide on Ni(111) surfaces at 100 K by HREELS and TPD and reported vibrational bands for acetonitrile at 1680–1700 cm^{-1} (low coverage) and 2240 cm^{-1} (high coverages). For methyl isocyanide, these features appear at 1760 cm^{-1} at low coverage and at 2160 cm^{-1} at high coverage. In both cases, the strongly red-shifted vibrational band was assigned as an η_2(C,N)-configuration with both the C and N atom of the nitrile and isocyanide group being bonded to the surface.[19] The adsorption geometry of nitriles was hypothesized to play a crucial rule in hydrogenation of nitrile compounds. A combined theoretical and FTIR study on acetonitrile hydrogenation to ethyl amine on Pt nanoparticles supported on Al_2O_3 by Vogt et al.[20] proposed η_2(C,N) adsorption configuration for chemisorbed nitriles and identified an imine species as the key reaction intermediate.

Thus, formation of two possible surface species was hypothesized in previous experimental reports on structurally similar molecules containing a nitrile or an isocyanide group. For the most of investigated surfaces,[9a,c–g,i-k,m,19] the adsorption configuration of the CN entity – either in nitrile or isocyanide compounds – was discussed to be oriented nearly parallel to the metal surface. Most of the authors hypothesized a η_2(C,N) adsorption configuration with both C and N atoms establishing σ bonds with the underlying metal. At increasing coverage, a more upright adsorption configuration was reported for the most investigated systems. These general observations are in a good agreement with the adsorption behavior of AC deduced from the IR spectra shown in Figure 3. It should be noted, however, that on the pristine Pd(111) surface no vibrational peaks in the range 1600–1750 cm^{-1} were observed in our work, which were interpreted in the earlier studies as imine –C=N species formed due to the strong interaction with the underlying metal and/or donation of the electron density from the metal to the C≡N bond. In the following, we will demonstrate and discuss formation of imine-like species on H-precovered Pd(111).

Adsorption of allyl cyanide on Pd(111) in the temperature range 100–250 K

As a next step, adsorption of allyl cyanide was investigated on pristine Pd(111) in the temperature range from 100 to 250 K at sub-monolayer coverages. For each temperature, the surface was exposed to 4.3 10^{14} molecules·cm^{-2} allyl cyanide. Note that the identical exposure does not result in the same surface coverages at different surface temperatures as the sticking coefficients may vary as a function of temperature.

Figure 4 shows the IR spectra obtained for this experimental series. At 100 K, intense vibrational bands at 1648 (ν(C=C)), 1419 ($\delta_{as}(CH_2)$), 990 (ω_{oop}(=CH)), 934 (ω_{oop}(=CH_2)), 915 (ν(C–C)/ν(C–CN)) cm^{-1} are visible at this particular exposure, while neither noticeable bands in the ν(CH_x) nor in ν(C≡N) regions could be observed, most likely due to MSSR. The combination of these observations suggests that the nitrile group of AC is

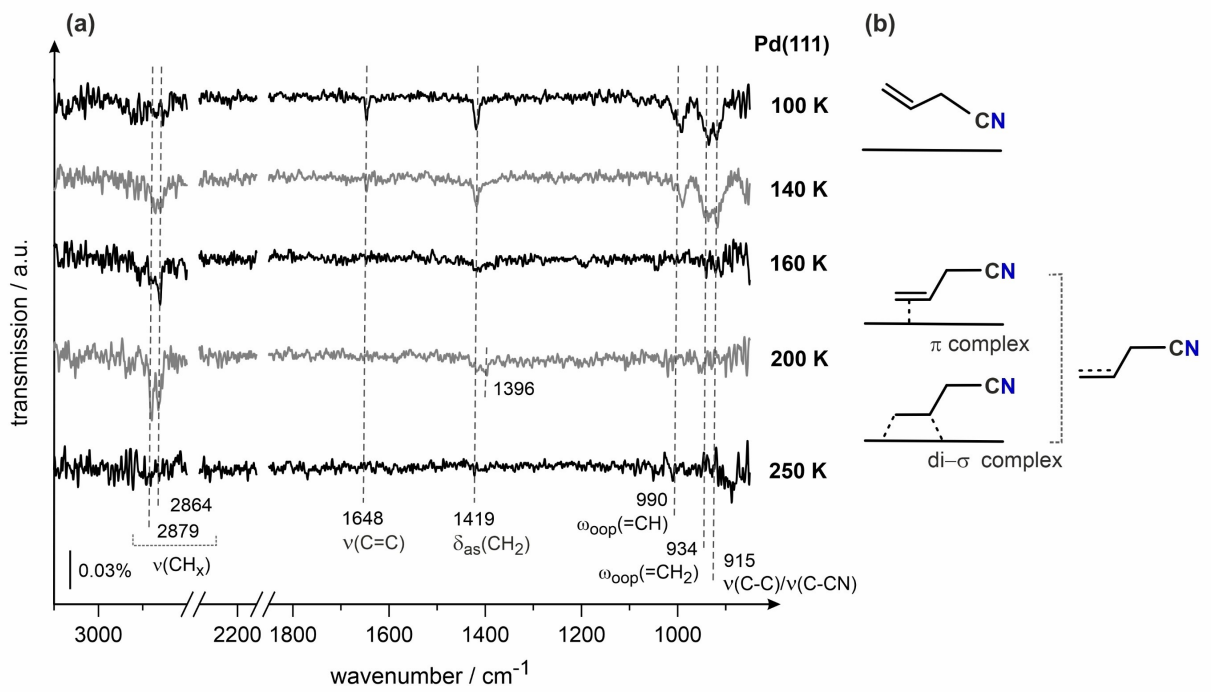

Figure 4. IR spectra of AC obtained on Pd(111) at submonolayer coverages in the temperature range 100–250 K. AC was dosed at a flux of $7.2 \cdot 10^{12}$ molecules·cm^{-2}·s^{-1} ; the total AC exposure amounts to $4.3 \cdot 10^{14}$ molecules·cm^{-2}. Acquisition temperatures are indicated next to the spectra.

oriented nearly parallel to the surface, while the C=C bond is tilted with respect to the surface plane.

Only minor changes occur transition to 140 K: the band at 1648 cm^{-1} (ν(C=C)) loses some intensity compared to the out-of-plane modes of the vinyl H-atoms (ω_{oop}(=CH) and ω_{oop}-(=CH_2)), which are related to the same functional group of the molecule. That observation indicates that the C=C bond is still present in the molecular species but the orientation of the vinyl group becomes more parallel with respect to the surface than at 100 K resulting in higher relative intensity of the out-of-plane modes. Importantly, two vibrational bands appear at 2879 and 2864 cm^{-1}, which is a typical range for C–H stretching vibrations in alkanes.[18] Note that the vibrational bands at these frequencies do not appear in the multilayer and therefore cannot be related simply to the –CH_2– groups of the originally deposited AC. With increasing temperature (160–200 K), these new vibrational bands grow in intensity, while the bands associated with the vinyl group at 1648 (ν(C=C)), 990 (ω_{oop}-(=CH)) and 934 (ω_{oop}(=CH_2)) vanish. The absence of both in-plane (ν(C=C)) and out-of-plane vibrations related to the vinyl group most likely indicates that the C=C bond is either strongly rehybridized or does not exist anymore under these temperature conditions. Also the original –CH_2– group is affected by temperature-induced structural changes since the band at 1419 cm^{-1} (δ_{as}(CH_2)) strongly decreases in intensity and a small new band at 1396 cm^{-1} evolves, which is most likely related to a similar C–H deformation vibration of the CH_x entity formed in the modified AC surface species.

Based on these spectroscopic observations, it is impossible to undoubtedly deduce the chemical composition of AC-related species formed in the temperature range 140–200 K on pristine Pd(111). Vanishing of the C=C bond can originate either *(i)* from formation of the π-complex with the intact C=C bond being nearly parallel oriented to the metal surface or *(ii)* due to formation of a di-σ complex, in which each C atom forms a covalent bond to the underlying Pd atom, so that the C=C bond does not exist anymore. There is an ongoing debate on this issue in the literature for different types of olefins, which is – to the best of our knowledge – not finally resolved.[17] Specifically, similar evolution of C=C-related spectroscopic signatures was reported by Lee et al.[18] for adsorption of simple olefins – butenes – on Pt(111) and assigned to the formation of a di-σ-bonded surface intermediate. On the other hand, notable changes of the spectral region related to the CH_x deformation vibrations (bands at 1419 and 1396 cm^{-1}) suggest that also the methylene group of original AC is strongly affected in the high temperature range. Similar behavior was previously reported for a close type of nitrile compounds – alkoxybenzonitriles, in which strong changes of the CH_x deformation vibrational bands were detected and linked to self-assembling of these species graphene.[21] In our previously published work, we reported that also AC self assembles in the 2D layers in the high temperature region and deduced the precise atomistic model of these adsorption layers (for more details, see[8]). In view of this fact, it is likely that also the changes of the vibrational bands at 1419 and 1396 cm^{-1} observed in this study are associated with the self-assembling process, in which strong intermolecular interactions keeping the molecular species together might be responsible for the observed behavior.

Above 250 K, no IR vibrational can be detected on the surface, even though that according to the STM data, the surface is almost completely covered by AC.[8] Vanishing of all vibrational bands occurs most likely due to the nearly flat orientation of all main bands parallel to the surface plane, making them not detectable by IRAS due to MSSR.[16] Potentially, also some hydrogen atoms of AC can be stripped off at elevated temperatures, however, their desorption from Pd cannot be observed experimentally in this temperature range since the barrier for desorption of surface-adsorbed H can be overcome only above 300 K. It should be noted that the ability of the AC-derivatives to efficiently diffuse at elevated temperatures, which is proven by formation of the long-range ordered structures (2D self-assembled layers), allow us to exclude a high degree of dissociation rather safely in these adsorbates. Indeed, if H would be stripped off the molecules in substantial amounts, it should form surface species strongly bound to Pd, which are most likely not capable to efficiently diffuse and strongly rearrange to form large areas of self-assembled 2D layers that are observed experimentally.

Figure 4b shows the proposed configuration of the AC species adsorbed on pristine Pd(111) in the temperature range 100–250 K. At the lowest temperatures, the nitrile group it oriented nearly parallel to the metal surface, while the C=C bond is inclined. The latter conclusion is based on the simultaneous observation of the stretching vibration of the C=C bond as well as wagging out-of-plane vibrations related to the vinyl group. In the range 140–160 K, a transition to new surface species occurs, in which the C=C bond seems to be highly rehybridized, forming most likely either di-σ or π-bonded complexes, in which all main bonds are oriented flat with respect to the surface. As reflection of these considerations, we replace the C=C double bond via the dotted line between two C atoms. Above 250 K no spectroscopic signatures of adsorbed species were detected by IRAS, while in STM AC coverages close to a monolayer were detected. These observations suggest a flat-lying adsorption configuration of all main bonds in AC-derivatives formed at this temperature.

Adsorption of allyl cyanide on H-precovered Pd(111) in the temperature range 100–250 K

To further understand the chemical transformation of AC in presence of co-adsorbed H and the state of the ligand layer under the reaction conditions – at elevated temperatures and under continuous H_2 exposure – adsorption of AC on the H-containing Pd(111) was investigated in the same temperature range as described in the previous section. Figure 5 shows the IR spectra obtained on H-containing Pd(111) surface at successively increasing temperatures.

In the temperature range 100–140 K, AC adsorbed on H-precovered surface still retains a number of peaks typical of molecularly adsorbed AC: 1648 (ν(C=C)), 1419 ($\delta_{as}(CH_2)$), 990 (ω_{oop}(=CH)), 934 (ω_{oop}(=CH_2)) and 915 cm^{-1} (ν(C–C)/ ν(C–CN)).[13a] Importantly, a new vibrational band at 1755 cm^{-1} appears on H-precovered Pd(111), which is present neither in

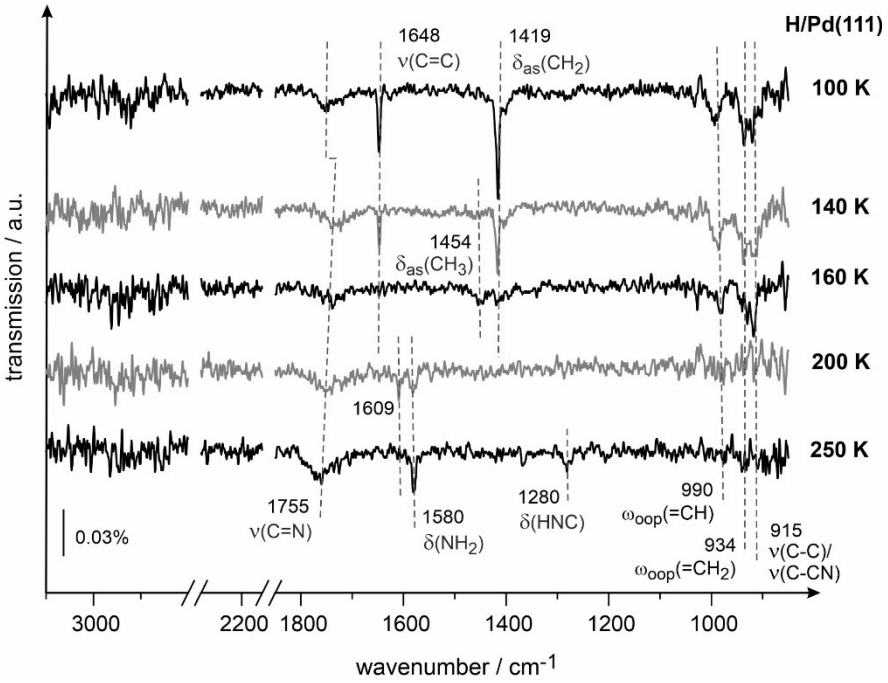

Figure 5. IR spectra of AC obtained on H-containing Pd(111) at submonolayer coverages in the temperature range 100–250 K. AC and H_2 were continuously dosed via independent molecular beams at fluxes $7.2 \cdot 10^{12}$ molecules·cm^{-2}·s^{-1} and $8.5 \cdot 10^{14}$ molecules·cm^{-2}·s^{-1}, respectively. Prior to the deposition of AC, H_2 was continuously dosed for 10 min onto the surface. The total AC exposure is $4.3 \cdot 10^{14}$ molecules·cm^{-2}. Surface temperatures are indicated next to the spectra.

multilayer nor in the gas phase AC.[13a] As discussed above, the bands appearing in the vibrational range 1600–1770 cm^{-1} after adsorption of structurally similar nitriles and isocyanides were previously attributed to the imine –C=N species both in experimental[9a,d,f,22] and theoretical[9k] studies. Following this assignment, we attribute the new band at 1755 cm^{-1} to the imine-like species, in which the original C≡N triple bond is partially reduced to a C=N double bond. It should be noted that the vibrational band is located at a similar frequency on Pd(111) precovered with D instead of H. Figure 6 shows a series of the related IR spectra obtained at 250 K on the D-precovered surface at different AC coverages, in which the evolution of the band at 1755 cm^{-1} can be observed, which has the same frequency as measured on the H-covered surface. This observation suggests that the frequency of the newly formed imine (C=N) group is not strongly affected by the nature of hydrogen isotope (H vs. D) inserted into the C≡N bond to form imine species.

Generally, two possible types of imine species evolving on H-precovered surface at 100–140 K are possible, which can be formed in two competing reaction pathways as shown in Figure 7. The species formed in the pathway 1 are bound through the N atom to Pd, producing the –C=N···Pd entity, which will be denoted later as N-butenylimine species (or

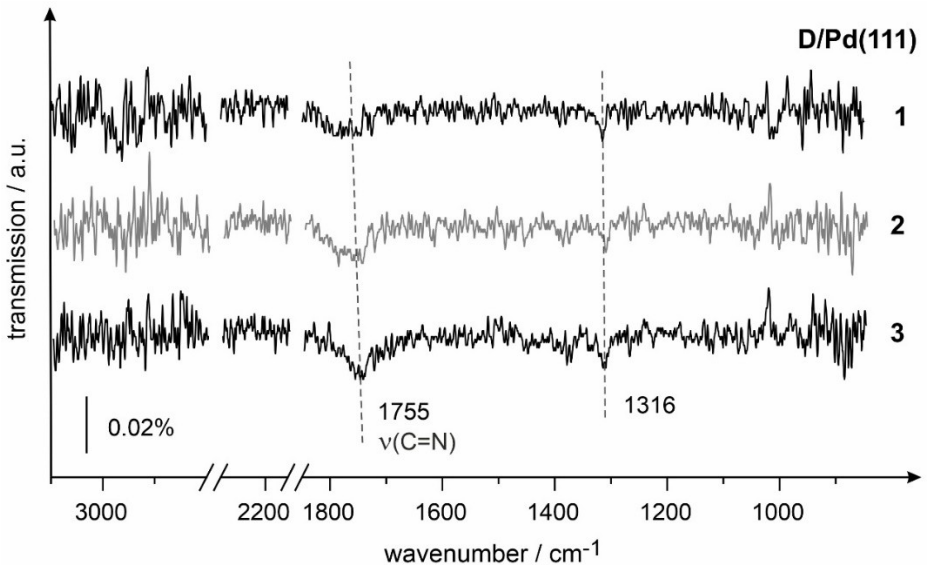

Figure 6. IR spectra of AC obtained at 250 K on D-containing Pd(111). AC and D_2 were continuously dosed via independent molecular beams at fluxes $7.2 \cdot 10^{12}$ molecules·cm^{-2}·s^{-1} and $8.5 \cdot 10^{14}$ molecules·cm^{-2}·s^{-1}, respectively. Prior to the AC exposure, the surface was exposed to D_2 for 10 min. The total AC exposures are: (1) $2.2 \cdot 10^{14}$, (2) $4.3 \cdot 10^{14}$, (3) $1.1 \cdot 10^{15}$ molecules·cm^{-2}.

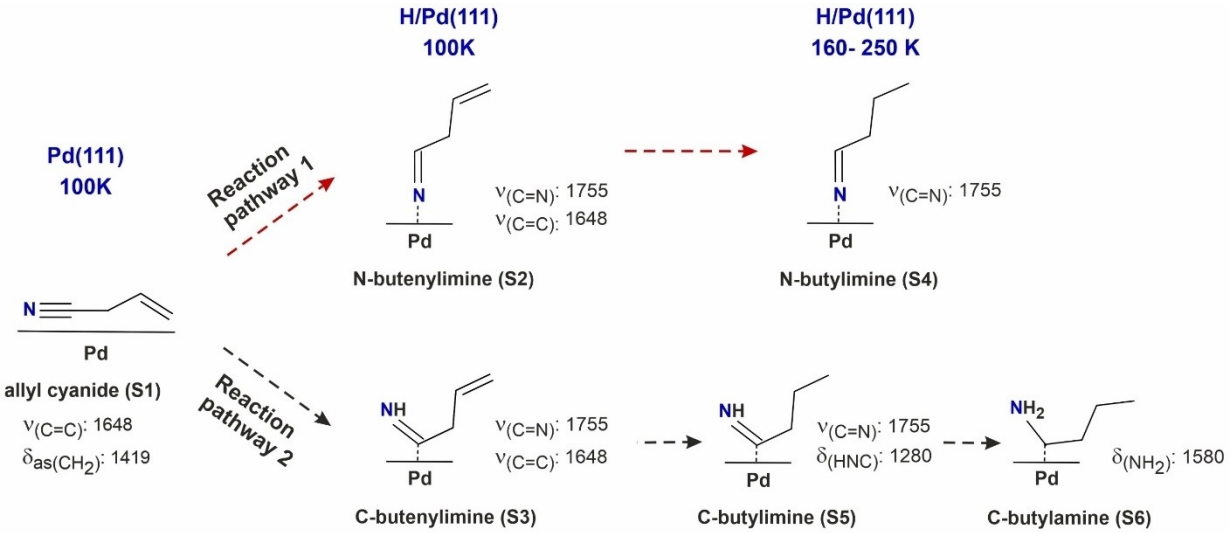

Figure 7. Proposed adsorbate structures and chemical transformation of AC on pristine and H-containing Pd(111). Reaction pathways 1 and 2 show the proposed partial hydrogenation steps in different temperature ranges. The frequencies of the vibrational bands used for assignment of the individual surface species are indicates next to the corresponding structures.

species S2). In the alternative reaction pathway 2, the species S3 is formed, which is connected to Pd via the C atom and will be denoted as C-butenylimine species. The geometric configuration of AC adsorbed on pristine Pd(111) at 100 K (as discussed above) is also shown in Figure 7 and denoted as species S1. It is important to note, that the spectroscopic signature of both proposed imine species S2 and S3 is the same and comprises two characteristic vibrations: the band at 1755 cm^{-1} related to the imine fragment –C=N and the band at 1648 cm^{-1} assigned to the C=C stretching vibration (ν(C=C)). The latter band clearly indicates that the C=C double bond is preserved in the species formed at 100–140 K at H-precovered Pd(111) surface.

At 160 K (Figure 5), the peaks at 1648 (ν(C=C)) and 1419 ($\delta_{as}(CH_2)$) cm^{-1} disappear, while a new peak at 1454 cm^{-1} corresponding to the CH_3 deformation vibration ($\delta_{as}(CH_3)$) evolves. The combination of these observations might suggest that the C=C bond becomes hydrogenated in this temperature range and a new terminal -CH_3 group appears. It should be noted, however, that the bands at 990 (ω_{oop}(=CH)) and 934 (ω_{oop}(=CH_2)) cm^{-1} are still visible in the spectra, even though they are strongly reduced in the intensity as compared to the low temperature regime. Most likely, a stepwise transition from the unsaturated butenylimine species (CH_2=CH–CH_2–CN) to saturated butylimine species (CH_3–CH_2–CH_2–CN) occurs in this temperature range and a combination of these both surface species temporarily exists on the surface. This hypothesis would explain the coexistence of the new band at 1454 cm^{-1} related to the terminal CH_3 group, which can originate only from hydrogenation of the C=C bond on one hand, and the bands at 990 (ω_{oop}(=CH)) and 934 (ω_{oop}(=CH_2)) cm^{-1} suggesting that some surface species still preserve their C=C bond, on the other hand. At the temperatures above 160 K, all vibrations related to C=C double bond (ν(C=C), ω_{oop}(=CH) and ω_{oop}(=CH_2)) completely vanish, suggesting that in the higher temperature range this transition is completed and all olefinic groups become fully hydrogenated (see spectra above 160 K in Figure 5). It should be emphasized that the conclusion on the hydrogenation of the C=C bond above 160 K is based on the combination of two observations: vanishing of the C=C stretching vibration (ν(C=C)) and disappearance of the bands related to the C–H out-of-plane wagging vibrations (ω_{oop}(=CH) and ω_{oop}(=CH_2)). As the dynamic dipole moments of these vibrational modes lie not in the same plane, their simultaneous disappearance cannot be related to the metal surface selection rule and therefore arises most likely from the hydrogenation of the C=C bond. This observation is in an agreement with earlier hydrogenation studies on simple olefins adsorbed on Pd(110) and Pd(111), where the onset of C=C bond hydrogenation was reported to occur around 160 K[23]

At 200 K (Figure 5), additional new bands appear at 1609 and 1580 cm^{-1}. Both bands lie in the vibrational region typical for deformation vibration of amino groups δ(NH_x). In previous studies, formation of vibrational bands in the range 1560–1616 cm^{-1} upon adsorption of simple amines at different transition metal surfaces was reported.[9h,m,24] Interestingly, both bands appear first at 200 K at comparable intensities. However, the band at 1609 cm^{-1} decreases in intensity at 250 K, while the band at 1580 cm^{-1} simultaneously grows (Figure 5), suggesting that these bands may be correlated as an intermediate (species related the band at 1609 cm^{-1}) and the final product (species related the band at 1580 cm^{-1}). Another observation pointing to the same hypothesis was made in a series of experiments shown in Figure 8. Here, the surface was continuously exposed to H_2, and to AC at different exposures (from $7.2\cdot10^{13}$ to $7.2\cdot10^{14}$ molecules·cm^{-2}). At the lowest exposures (spectra 2–3), the band at 1609 cm^{-1} dominates the spectrum, while the band at 1580 cm^{-1} is hardly seen. With increasing exposure, the band at 1609 cm^{-1} decreases in intensity and finally vanishes, while the band at 1580 cm^{-1} concomitantly grows and the eventually becomes the dominant band in the spectrum 5. This correlated behavior, which was observed as a function of both temperature (Figure 5) and the exposure (Figure 8), suggests that the species related to the band at 1609 cm^{-1} might be the surface precursor, which completely transforms into surface amines (-NH_2) exhibiting the band at 1580 cm^{-1} (δ(NH_2)). The exact chemical nature of the species related to the band at 1609 cm^{-1} is unclear yet. It should be a structurally similar species, containing an amino group, which can be for example adsorbed at a different adsorption sites or having a different local environment (e.g. different intermolecular interactions) than the species related the band at 1580 cm^{-1}. As a possible scenario, it can be hypothesized that the band at 1580 cm^{-1} can be related to the amine species, which are involved in intermolecular interactions with neighboring molecules and are formed at higher coverages, while the band at 1609 cm^{-1} can be rather associated with alone-standing amines present in the low coverage range. This hypothesis is in good agreement with the previous studies on intermolecular interactions of amines, in which the amine group was shown to be involved into hydrogen bonding with foreign molecules. Thus, for aniline/dimethyl sulfoxide (DMSO) complex the deformation vibration δ(NH_2) was observed to blue shift by 12 cm^{-1} per intermolecular hydrogen bond with a neighboring DMSO molecule.[25] Additionally, IR studies on intermolecular interactions of aniline in liquid phase revealed a blue-shift of 20–30 cm^{-1} for the NH_2 deformation vibration δ(NH_2) when aniline forms adducts with other aniline molecules.[26]

At 250 K, the spectra (Figure 5) show intense vibrational bands at 1755 (ν(–C=N)), 1580 (δ(NH_2)) and 1280 cm^{-1}. The latter band is new and was assigned in the previous theoretical study to the deformation vibration of the imine fragment H-N=C– in the hydrogenation of acetonitrile, which was calculated as one of the products in nitrile hydrogenation.[20] Following this assignment, we will denote this vibration as δ(HNC). It is important to emphasize that the calculated vibration at 1280 cm^{-1} is related to the fragment, in which a N=C exist and a H atom is attached to N. This fragment should be discriminated from the N-butenylimine species S2 shown in Figure 5, in which N is attached to Pd but not to a H atom.

Simultaneous appearance of the bands at 1755, 1580 and 1280 cm^{-1} means that both imine and amine species are formed and co-exist in this temperature range. It also suggests that at least two reaction pathways run in parallel to transfer

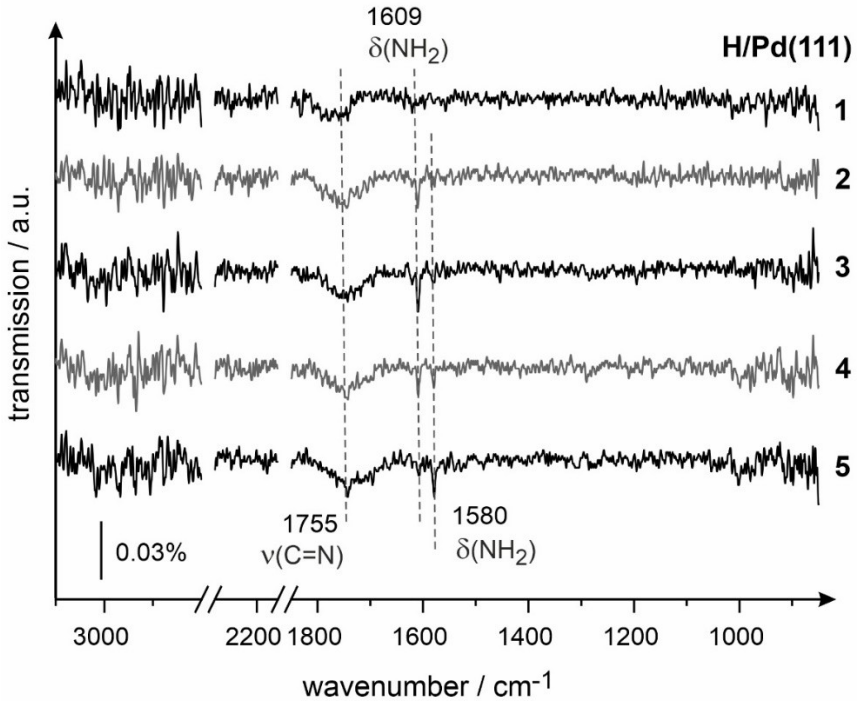

Figure 8. IR spectra of AC obtained on H-containing Pd(111) at 200 K. AC and H_2 were dosed via independent molecular beams at fluxes $7.2 \cdot 10^{12}$ molecules·cm^{-2}·s^{-1} and $8.5 \cdot 10^{14}$ molecules·cm^{-2}·s^{-1}, respectively. AC exposures are: (1) $7.2 \cdot 10^{13}$, (2) $2.9 \cdot 10^{14}$, (3) $3.6 \cdot 10^{14}$, (4) $4.3 \cdot 10^{14}$, (5) $7.2 \cdot 10^{14}$ molecules·cm^{-2}.

the originally deposited AC to co-existing imine and amine surface species.

It is also important to emphasize that the bands at 1580 ($\delta(NH_2)$) and 1280 (δ(HNC)) cm^{-1} show a strongly correlated evolution upon prolonged H_2 exposure at a constant temperature. Figure 9 displays a series of IR spectra obtained at 250 K and a continuous exposure of H_2 during different times. At the lowest H_2 exposure (spectrum 1–2), both bands at 1580 and 1280 cm^{-1} are clearly visible. While the exposure increases (spectra 5–6), a strong simultaneous intensity decrease of both bands is observed, which occurs in a correlated way. The possible reasons of this behavior will be discussed in the following.

Figure 7 shows the proposed model for the competing reaction pathways in successive AC hydrogenation, which is consistent with all spectroscopic observations. For all proposed species, the most important vibrational bands employed for assignment are displayed next to the proposed structure.

At 100 K, AC adsorbed on pristine Pd(111) exhibits an adsorption configuration with the C=C bond is inclined with respect to the surface plane (and therefore visible in IRAS), while the CN group is oriented nearly parallel to the surface (species S1). Upon adsorption of AC on H-precovered surface at 100 K, a fraction of the surface species forms the imine group (–C=N) giving rise to a characteristic vibrational band at 1755 cm^{-1}. The formed butenylimine species still contain the C=C double bond (band at 1648 cm^{-1}) and can be principally bound to Pd either via the N atom (N-butenylimine, S2 species) or via the C atom (C-butenylimine, S3 species). Both types of butenylimine species can undergo further hydrogenation steps, which can be divided into two competing reaction pathway resulting in formation of saturated N-butylimine (pathway 1) and C-butylamine species (pathway 2). In the first pathway, the N-butenylimine species (S2) is hydrogenated at the C=C bond producing the N-butylimine (S4) species in the temperature range 160–250 K. This process is accompanied by stepwise disappearance of all vibrational signatures characteristic for C=C bonds (bands at 1648, 990 and 934 cm^{-1}). In the second pathway, the C–butenylimine (S3) species become also hydrogenated at the C=C bond in the same temperature range forming C-butylimine species (S5), which exhibits a combination of characteristic bands at 1755 (C=N) and 1280 (HNC) cm^{-1}. In contrast to the first reaction pathway, further hydrogenation steps occur at the imine group of S5 species: the imine group becomes hydrogenated to amine forming C-butylamine species (S6), showing a typical deformation vibration of the amino groups at 1580 cm^{-1} ($\delta(NH_2)$). It is important to emphasize that the species S5 and S6 co-exist on the surface and evolve in a correlated fashion: they appear in the same temperature range and both disappear in a correlated way upon prolonged H_2 exposure in the course of the reaction (Figure 9). Note that the characteristic vibrational bands used to assign the species S5 and S6 (δ(HNC) at 1280 and $\delta(NH_2)$ at 1580 cm^{-1}, correspondingly) cannot originate from the same surface species. On the other hand, the nearly simultaneous evolution of these species with increasing temperature and simultaneous disappearance upon prolonged exposure to H_2 suggest that the species S5 and S6 are strongly correlated, most likely as a precursor (S5) and

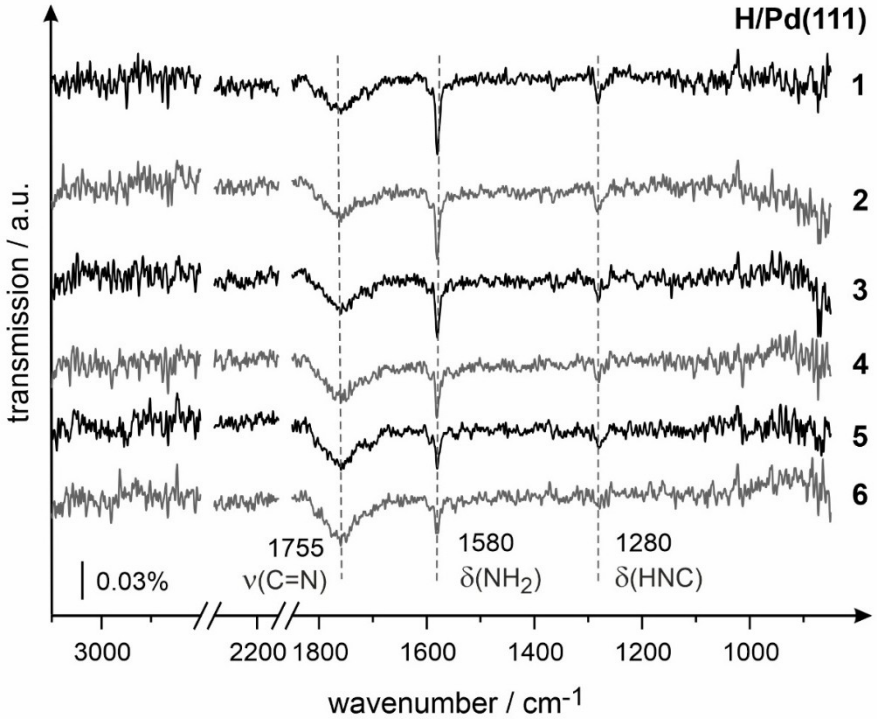

Figure 9. IR spectra of AC obtained at H-containing Pd(111) at 250 K. AC and H_2 were dosed via independent molecular beams at fluxes $7.2 \cdot 10^{12}$ molecules$\cdot$cm$^{-2}\cdot$s^{-1} and $8.5 \cdot 10^{14}$ molecules$\cdot$cm$^{-2}\cdot$s^{-1}, respectively. AC exposure is 1.0 L, H_2 beam was continuously running. Spectra 1–6 correspond to different H_2 exposure times: (1) 0, (2) 135, (3) 270, (4) 405, (5) 540, (6) 675 sec.

the product (S6). These considerations are reflected in the proposed reaction mechanism for the reaction pathway 2, showing that the species C-butylimine species (S5) is the direct precursor to the C-butylamine species (S6).

Summarizing, the combination of all spectroscopic data allows us to conclude that the originally adsorbed AC species S1 undergo successive hydrogenation steps along two competing reaction pathways: in the first pathway, the N-butylimine (S4) species are formed, while the second pathway leads to the formation of the mixture of C-butylimine (S5) and C-butylamine (S6) species. It is important to note that under the hydrogenation reaction conditions (prolonged H_2 exposure, temperatures around 250 K), only one type of species – N-butylimine (S4) – remains present on the catalytic surface, while the other two species – C-butylimine (S5) and C-butylamine (S6) – readily disappear from the surface after prolonged H_2 exposure (see Figure 9). Most likely, the surface species S5 and S6 become fully hydrogenated to molecular butylamine, which is able to desorb. This observation suggests that the active ligand layer, acting in the reaction of chemoselective hydrogenation of acrolein over AC-functionalized Pd(111) catalyst, consists of the stable N-butylimine (S4) species formed in the first pathway. In contrast, the mixture of the unstable C-butylimine (S5) and C-butylamine (S6) species are the spectator species, which readily disappear in the early stages of the reaction.

It should be also noted that the existence of two reaction pathways most likely originates from different adsorption configurations of butenylimine species S2 and S3. While attached to Pd through the N-atom, the N-butenylimine (S2) species remain protected from further hydrogenation of the imine part of the molecule. In case of C-butenylimine (S3) adsorbates, the non-bonded N-atom can be further attacked by hydrogen and become hydrogenated to amine as observed for the second reaction pathway.

Formation of the stable ligand layer consisting of S4 species turns Pd(111) surface highly active and nearly 100% selective for acrolein hydrogenation.

The different surface species formed as a result of partial AC hydrogenation should be verified in the future theoretical studies to obtain deeper insights in the competing reaction pathways of AC leading to formation of a highly active ligand layer. The structures of all AC-related surface species deduced from the above discussed spectroscopic information provide important starting structures for the future computational studies.

Conclusions

Adsorption of allyl cyanide on pristine and H-containing Pd(111) was investigated by a combination of IRAS, molecular beam techniques and theoretical calculations at B3LYP level.

On pristine Pd(111) surface allyl cyanide adsorbs in the configuration, in which the nitrile groups are oriented parallel to the surface plane, while the C=C bond is tilted. With increasing temperature, the spectroscopic observations suggest

that strong rehybridization of the C=C bond occurs, which might result in formation of π- or di-σ-bonded surface species on the olefinic part of the molecule.

In presence of hydrogen, allyl cyanide undergoes dramatic changes in both the chemical structure of the adsorbed species and their adsorption configuration. At 100 K, allyl cyanide converts to unsaturated imine species – butenylimine – exhibiting characteristic vibrational bands at 1755 cm^{-1} related to the –C=N fragment and at 1648 cm^{-1} corresponding to the C=C bond. At increasing temperatures, these species can undergo two competing reaction pathways, including stepwise partial hydrogenation at different functional groups. In the first pathway, the C=C bond becomes hydrogenated in the temperature range 160–200 K to produce saturated imine – N-butylimine species – which remain stable under the reaction conditions up to at least 250 K. We hypothesized that these species are strongly bound to Pd via the N-atom as (–C=N···Pd), which protects the imine group from further hydrogenation. In the competing reaction pathway, the butenylimine species are fully hydrogenated to butyl amine, which desorbs from the surface as molecular species after prolonged hydrogen exposure. In this pathway, both C=C and C=N groups become hydrogenated in the temperature range 160–200 K (for C=C bond) and 200–250 K (for C=N bond). Based on all spectroscopic observations, we propose a mechanistic model explaining the evolution of stable saturated butylimine species resulting from the first reaction pathway and the unstable butylamine adsorbates formed in the second reaction pathway. According to this model, the originally adsorbed allyl cyanide can form butenylimine species in two different configurations: bound via the N- vs. C-atom of the original nitrile group. While attached to Pd through the N-atom, the butenylimine species remain protected from further hydrogenation of the imine part of the molecule. In the opposite case of bonding through the C-atom, the non-bonded N-atom can be further attacked by hydrogen and become hydrogenated to amine as observed for the second reaction pathway. Under the reaction conditions relevant for chemoselective hydrogenation of acrolein (250 K, high hydrogen flux), only the strongly bound N-butylimine species remain on the surface and act as a ligand layer, while the butylamine species desorb.

Obtained microscopic-level insights into the chemical structure of adsorbates formed on AC-functionalized Pd surface and their dynamic changes under the reaction conditions provide important information for purposeful modification of metal catalysts by functionalization with ligand layers to achieve better catalytic performance.

Acknowledgements

This work has been supported by the German Science Foundation (DFG, Grant SCHA 1477/6-1, INST 257/543-1 FUGG). Open Access funding enabled and organized by Projekt DEAL.

Conflict of Interest

The authors declare no conflict of interest.

Keywords: allyl cyanide · infrared spectroscopy · ligand-directed catalysis · reaction mechanisms · reactive intermediates

[1] R. Dennington, T. A. Keith, J. M. Millam, *GaussView, Version 6.1*, Semichem Inc., Shawnee Mission, KS, 2016.
[2] T. H. Rod, J. K. Nørskov, *Surf. Sci.* **2002**, *500*, 678–698.
[3] a) J. P. Collman, Z. Wang, A. Straumanis, M. Quelquejeu, E. Rose, *J. Am. Chem. Soc.* **1999**, *121*, 460–461; b) M. S. Taylor, E. N. Jacobsen, *Angew. Chem. Int. Ed.* **2006**, *45*, 1520–1543.
[4] a) S. T. Marshall, M. O'Brien, B. Oetter, A. Corpuz, R. M. Richards, D. K. Schwartz, J. W. Medlin, *Nat. Mater.* **2010**, *9*, 853–858; b) F. Meemken, A. Baiker, *Chem. Rev.* **2017**, *117*, 11522–11569; c) A. J. Gellman, W. T. Tysoe, F. Zaera, *Catal. Lett.* **2015**, *145*, 220–232; d) P. Gallezot, D. Richard, *Catal. Rev. Sci. Eng.* **1998**, *40*, 81–126; e) S. T. Marshall, J. W. Medlin, *Surf. Sci. Rep.* **2011**, *66*, 173–184.
[5] a) P. Sonstrom, M. Baumer, *Phys. Chem. Chem. Phys.* **2011**, *13*, 19270–19284; b) I. Schrader, S. Neumann, A. Šulce, F. Schmidt, V. Azov, S. Kunz, *ACS Catal.* **2017**, *7*, 3979–3987; c) S. Kunz, *Top. Catal.* **2016**, *59*, 1671–1685; d) L. Rodríguez-García, K. Hungerbühler, A. Baiker, F. Meemken, *ACS Catal.* **2017**, *7*, 3799–3809; e) C.-H. Lien, J. W. Medlin, *J. Catal.* **2016**, *339*, 38–46; f) S. H. Pang, J. W. Medlin, *J. Phys. Chem. Lett.* **2015**, *6*, 1348–1356; g) G. J. Hutchings, F. King, I. P. Okoye, M. B. Padley, C. H. Rochester, *J. Catal.* **1994**, *148*, 453–463; h) M. E. Chiu, G. Kyriakou, F. J. Williams, D. J. Watson, M. S. Tikhov, R. M. Lambert, *Chem. Commun.* **2006**, 1283–1285; i) R. A. Sheldon, H. van Bekkum, in *Fine Chemicals through Heterogeneous Catalysis*, Wiley-VCH Verlag GmbH, **2007**, pp. 351–471; j) S. Attia, M. C. Schmidt, C. Schröder, S. Schauermann, *ACS Catal.* **2019**, *9*, 6882–6889; k) S. Attia, M. C. Schmidt, C. Schröder, J. Weber, A.-K. Baumann, S. Schauermann, *J. Phys. Chem. C* **2019**, *123*, 29271–29277; l) S. Attia, E. J. Spadafora, J. Hartmann, H.-J. Freund, S. Schauermann, *Rev. Sci. Instrum.* **2019**, *90*, 053903; m) S. Attia, E. J. Spadafora, M. C. Schmidt, C. Schröder, A.-K. Baumann, S. Schauermann, *Phys. Chem. Chem. Phys.* **2020**, *22*, 15696–15706; n) M. C. Schmidt, S. Attia, C. Schröder, A.-K. Baumann, P. Pessier, S. Schauermann, *J. Phys. Chem. C* **2020**, *124*, 14262–14271; o) K.-H. Dostert, C. P. O'Brien, F. Ivars-Barceló, S. Schauermann, H.-J. Freund, *J. Am. Chem. Soc.* **2015**, *137*, 13496–13502; p) C. P. O'Brien, K.-H. Dostert, S. Schauermann, H.-J. Freund, *Chem. Eur. J.* **2016**, *22*, 15856–15863; q) K.-H. Dostert, C. P. O'Brien, F. Mirabella, F. Ivars-Barceló, S. Attia, E. Spadafora, S. Schauermann, H.-J. Freund, *ACS Catal.* **2017**, 5523–5533; r) S. Attia, M.-C. Schmidt, C. Schröder, P. Pessier, S. Schauermann, *Angew. Chem. Int. Ed.* **2018**, *57*, 16659–16664.
[6] W. Binghui, H. Huaqi, Y. Jing, Z. Nanfeng, F. Gang, *Angew. Chem. Int. Ed.* **2012**, *51*, 3440–3443.
[7] a) J. B. Ernst, S. Muratsugu, F. Wang, M. Tada, F. Glorius, *J. Am. Chem. Soc.* **2016**, *138*, 10718–10721; b) J. B. Ernst, C. Schwermann, G.-i. Yokota, M. Tada, S. Muratsugu, N. L. Doltsinis, F. Glorius, *J. Am. Chem. Soc.* **2017**, *139*, 9144–9147.
[8] C. Schröder, M. C. Schmidt, P. A. Haugg, A.-K. Baumann, J. Smyczek, S. Schauermann, *Angew. Chem. Int. Ed.* **2021**, *60*, 16349–16354.
[9] a) M. E. Kordesch, W. Stenzel, H. Conrad, *Sur. Sci.* **1988**, *205*, 100–116; b) M. E. Kordesch, T. Lindner, J. Somers, W. Stenzel, H. Conrad, A. M. Bradshaw, G. P. Williams, *Spectr. Acta .A Mol. Spec.* **1987**, *43*, 1561–1566; c) T. Szilágyi, *Appl. Surf. Sci.* **1988**, *35*, 19–26; d) B. A. Sexton, N. R. Avery, *Surf. Sci.* **1983**, *129*, 21–36; e) S. Semancik, G. L. Haller, J. T. Yates, *J. Chem. Phys.* **1983**, *78*, 6970–6981; f) K. Murphy, S. Azad, D. W. Bennett, W. T. Tysoe, *Surf. Sci.* **2000**, *467*, 1–9; g) N. R. Avery, T. W. Matheson, *Surf. Sci.* **1984**, *143*, 110–124; h) Y. Ren, D. Esan, I. Waluyo, J. D. Krooswyk, M. Trenary, *J. Phys. Chem. C* **2017**, *121*, 9424–9432; i) J. Raskó, J. Kiss, *Catal. Lett.* **2006**, *109*, 71–76; j) E. C. Ou, P. A. Young, P. R. Norton, *Surf. Sci.* **1992**, *277*, 123–131; k) S. Katano, E. Herceg, M. Trenary, Y. Kim, M. Kawai, *J. Phys. Chem. B* **2006**, *110*, 20344–20349; l) D. Jentz, M. Trenary, X. D. Peng, P. Stair, *Surf. Sci.* **1995**, *341*, 282–294; m) D. Jentz, H. Celio, P. Mills, M. Trenary, *Surf. Sci.* **1995**, *341*, 1–8.
[10] W. Erley, J. C. Hemminger, *Surf. Sci.* **1994**, *316*, L1025-L1030.
[11] S. Attia, E. J. Spadafora, J. Hartmann, H. J. Freund, S. Schauermann, *Rev. Sci. Instrum.* **2019**, *90*, 053903.
[12] M. J. Frisch, et al., *Gaussian 16 Rev. C.01*, Wallingford, CT, 2016.

[13] a) J. R. Durig, G. A. Guirgis, A. S. Drew, *J. Raman Spectrosc.* **1994**, *25*, 907–921; b) A. L. Verma, *J. Molec. Spect.* **1971**, *39*, 247–254.
[14] Z. Getahun, C. Y. Huang, T. Wang, B. De Leon, W. F. DeGrado, F. Gai, *J. Am. Chem. Soc.* **2003**, *125*, 405–411.
[15] B. A. Lindquist, S. A. Corcelli, *J. Phys. Chem. B* **2008**, *112*, 6301–6303.
[16] F. Hoffmann, *Surf. Sci. Rep.* **1983**, *3*, 107–192.
[17] F. Zaera, *ACS Catal.* **2017**, *7*, 4947–4967.
[18] I. Lee, F. Zaera, *J. Phys. Chem. C* **2007**, *111*, 10062–10072.
[19] C. M. Friend, E. L. Muetterties, J. Gland, *J. Phys. Chem.* **1981**, *85*, 3256–3262.
[20] L. Vogt, E. Schulte, S. Collins, P. Quaino, *Top. Catal.* **2019**, *62*, 1076–1085.
[21] H. D. Castillo, J. M. Espinosa-Duran, J. R. Dobscha, D. C. Ashley, S. Debnath, B. E. Hirsch, S. R. Schrecke, M. H. Baik, P. J. Ortoleva, K. Raghavachari, A. H. Flood, S. L. Tait, *Chem. Commun.* **2018**, *54*, 10076–10079.
[22] R. D. Adams, D. A. Katahira, L. W. Yang, *Organometallics* **1982**, *1*, 231–235.
[23] a) S. Ohno, M. Wilde, K. Mukai, J. Yoshinobu, K. Fukutani, *J. Phys. Chem. C* **2016**, *120*, 11481–11489; b) A. Doyle, *J. Catal.* **2004**, *223*, 444–453.
[24] D. F. Johnson, Y. Wang, J. E. Parmeter, M. M. Hills, W. H. Weinberg, *J. Am. Chem. Soc.* **1992**, *114*, 4279–4290.
[25] C. Greve, E. T. Nibbering, H. Fidder, *J. Phys. Chem. B* **2013**, *117*, 15843–15855.
[26] H. Wolff, W. Hagedorn, *J. Phys. Chem.* **1980**, *84*, 2335–2337.

Manuscript received: September 7, 2021
Accepted manuscript online: October 5, 2021
Version of record online: October 27, 2021

